Available online at www.sciencedirect.com

SciVerse ScienceDirect

Procedia Engineering 47 (2012) 554 – 557

Procedia Engineering

www.elsevier.com/locate/procedia

Proc. Eurosensors XXVI, September 9-12, 2012, Kraków, Poland

# Homogeneity Analysis of a MEMS-based PZT Thick Film Vibration Energy Harvester Manufacturing Process

Anders Lei[a]*, Ruichao Xu[b], Louise M. Borregaard[b], Michele Guizzetti[b], Erik V. Thomsen[a]

[a]*Department of Micro- and Nanotechnology, Technical University of Denmark, DTU Nanotech, Building 345B, DK-2800 Kongens Lyngby, Denmark*

[b]*Meggitt A/S, Hejreskovvej 20, Kvistgaard 3490, Denmark*

**Abstract**

This paper presents a homogeneity analysis of a high yield wafer scale fabrication of MEMS-based unimorph silicon/PZT thick film vibration energy harvesters aimed towards vibration sources with peak vibrations in the range of around 300 Hz. A wafer with a yield of 91% (41/45 devices) has been characterized. Measurements of the open circuit voltage showed a relative difference of 32.6% between the standard deviation and average. Measurements of the capacitance and resonant frequency showed a relative difference between the standard deviation and average value of 4.3% and 2.9% respectively, thus indicating that the main variation in open circuit voltage performance is caused by varying quality factor. The average resonant frequency was measured to 333 Hz with a standard variation of 9.8 Hz and a harvesting bandwidth of 5-10 Hz. A maximum power output of 39.3 μW was achieved at 1 *g* for the best performing harvester.



*Keywords:* Energy harvesting; Vibration harvesting; MEMS; PZT; Thick film

## 1. Introduction

With the recent development in low power electronics and small-scale energy harvesters, the realization of small long-term autonomous wireless sensors seems to become increasingly realistic. The criterion for success for energy harvesters is that their size does not exceed the volume batteries would

* Corresponding author. Tel.: +45 4525 5700; fax: +45 4588 7762.
*E-mail address*: anders.lei@nanotech.dtu.dk.


doi:10.1016/j.proeng.2012.09.207

take up to supply the required power in the sensors lifetime. This can be well achieved using MEMS technology, however most applicable vibration sources have peak frequencies in the range of a few hundred Hz [1], which for classical MEMS devices are considered unusually low. To achieve these resonant frequencies, designs with high length to thickness ratios and relative large proof masses have been utilized, resulting in devices that are laterally large and fragile during the fabrication processes. Recently Lei *et al.* [2] presented a high performance MEMS-based PZT thick film vibration energy harvester Fig. 1(a). In [2], and as for a majority of other MEMS-based vibration energy harvesters reported [3], [4] only measurements for a single device is presented. Based on an identical fabrication process as in [2], resulting in a yield of ~91% (41/45), characterization of each device from a full wafer will be presented in this paper, hence giving a comprehensive assessment of the device uniformity.

## 2. Results

The characterization is carried out in the following way: initially, the capacitance together with RMS open circuit voltage ($V_{oc}$) and resonant frequency ($F_{res}$) is measured for all harvesters. Secondly, the RMS power output dissipated in a resistive load is measured for a number of representative chips.

Fig. 1(b) shows a map of the measured capacitance for the 41 fabricated harvesters listed as the wafer layout with rows and columns. The average measured capacitance is 5.638 nF with a standard deviation of 0.243 nF. The average capacitance corresponds to a dielectric constant of 842. The peak RMS $V_{oc}$ measured with an input RMS acceleration of 0.5 $g$ is seen in Fig. 2(a). The average $V_{oc}$ is 1.6 V with a standard deviation of 0.52 V. The resonant frequency at which peak $V_{oc}$ is obtained is mapped in Fig. 2(b). The average $F_{res}$ is measured to 333.3 Hz with a standard deviation of 9.8 Hz.

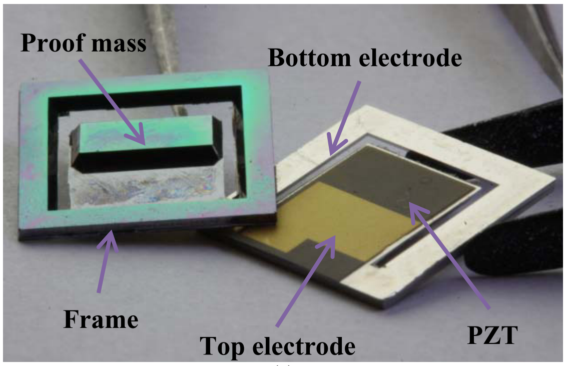


(a)

| | A | B | C | D | E | F | G |
|---|---|---|---|---|---|---|---|
| 1 | | 5.342 | 5.448 | 5.495 | 5.234 | 5.096 | |
| 2 | 5.336 | 5.640 | 5.693 | 5.679 | 5.600 | 5.506 | 5.343 |
| 3 | 5.139 | | 5.799 | 5.769 | 5.636 | 5.564 | 5.398 |
| 4 | 5.768 | 5.766 | 5.839 | 5.924 | | 5.724 | 5.004 |
| 5 | 5.789 | 5.868 | 5.884 | 5.924 | 5.934 | 5.896 | 5.449 |
| 6 | 5.765 | 5.958 | 5.671 | | 5.779 | 5.615 | 5.588 |
| 7 | | | 5.812 | 5.853 | 5.749 | 5.869 | |

[nF] 6 5.64 5

(b)

Fig. 1. (a) Photograph of the front and backside of the fabricated vibration energy harvester. (b) Characterization map of the measured PZT layer capacitance.

### 2.1. Load measurements

For the power output measurements a total of 10 representative harvester devices are selected. Three devices are selected from around each of the three quartiles ($Q_1$=1.17 V, $Q_2$=1.55 V and $Q_3$=2.08 V) of the $V_{oc}$ measurements, the last harvester selected is the one with highest $V_{oc}$ output. In Fig. 3(a) the iteratively found optimal resistive load ($R_{load}$) is listed for each of the selected harvesters together with the measured RMS power output ($P=V_{rms}^2/R_{load}$) for the three RMS accelerations 0.5 $g$, 0.75 $g$ and 1 $g$. The bandwidth is measured as full width at half maximum ($BW_{FWHM}$) at 0.5 $g$ acceleration and the total quality factor is calculated as $Q_{total}=F_{res}/BW_{FWHM}$. In Fig. 3(b) the results are outlined with power output at the three accelerations plotted for each of the 10 harvesters.

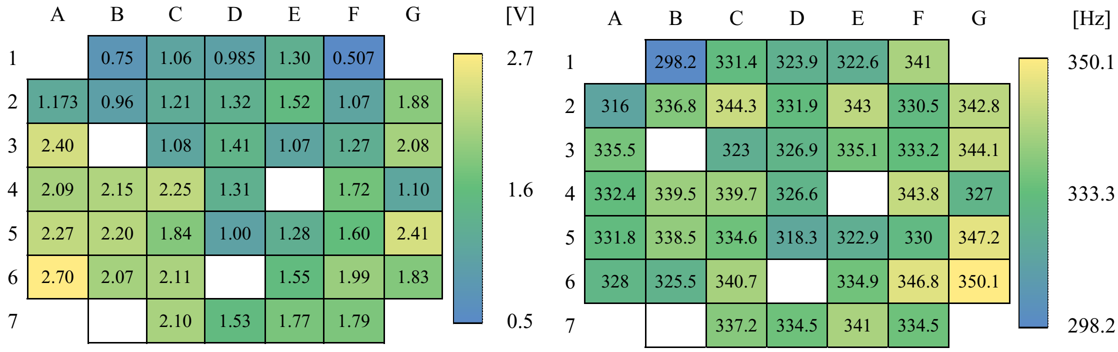


Fig. 2. (a) Map of the maximum measured RMS open circuit voltage during frequency sweeps with an input RMS acceleration of 0.5 *g*. (b) Map of the corresponding measured resonant frequency.

## 3. Discussion

Assuming that the porosity and thus the dielectric constant of the screen-printed PZT thick film is constant over the wafer, the variation in capacitance is an estimate of geometrical variations. The lateral dimensions of the capacitor are defined by the deposited electrodes which are controlled by lithography. It can therefore be assumed that the main contribution to the variation in capacitance is variations in thickness of the PZT thick film. Percentagewise, the standard deviation is 4.3% relative to the average value. This corresponds to a variation of 1.2 µm out of a PZT film thickness of 27 µm.

From an application point of view the main success criteria for a linear vibration energy harvester is the frequency match with the vibration source. $F_{res}$ is determined by mechanical properties with the cantilever thickness and distance from cantilever anchoring point to center of mass as the dominating geometrical parameters. The silicon part of the cantilever is determined accurately by the device layer thickness of the silicon-on-insulator wafer, and the capacitance characterization indicated a relatively small thickness variation of the PZT. The distance to the center of mass, width of the cantilever and mass of the proof mass are all determined by lithography. The standard deviation relative to the average measured $F_{res}$ is 2.9%. Ignoring the two lowest and highest measurements this value decreases to 2.2%. Since $F_{res}$ is proportional to the square root of the cantilever thickness cubed, the relative variation is expected to be higher, although the silicon part accounts for a significant part of the cantilever stiffness.

| | Chip | Load [kΩ] | $BW_{FWHM}$ [Hz] | $Q_{total}$ | RMS Power [µW] | | |
|---|---|---|---|---|---|---|---|
| | | | | | 0.5*g* | 0.75*g* | 1g |
| Peak | A6 | 150 | 5.00 | 65.9 | 12.5 | 25.0 | 39.3 |
| Q3 2.08V | G3 | 50 | 6.80 | 50.7 | 10.5 | 22.1 | 35.0 |
| | B4 | 50 | 6.80 | 49.7 | 9.6 | 21.3 | 35.8 |
| | B6 | 50 | 6.60 | 49.3 | 9.7 | 21.4 | 34.7 |
| Q2 1.55V | F5 | 50 | 8.20 | 40.1 | 6.7 | 15.7 | 25.7 |
| | D7 | 75 | 9.00 | 37.1 | 6.1 | 14.8 | 24.3 |
| | E6 | 75 | 8.50 | 39.2 | 5.5 | 13.1 | 22.5 |
| Q1 1.17V | C2 | 75 | 8.75 | 37.7 | 4.8 | 11.1 | 17.9 |
| | A2 | 75 | 8.20 | 38.4 | 5.1 | 10.9 | 15.3 |
| | C3 | 75 | 10.25 | 31.1 | 2.9 | 7.2 | 13.3 |

(a)

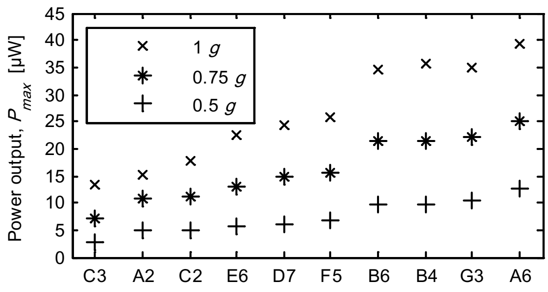


Fig. 3. (a) RMS power output measurements for 10 harvester devices representative for the 41 fabricated devices. Power is measured at three different RMS accelerations with the resistive load listed. Bandwidth ($BW_{FWHM}$) and total quality factor ($Q_{total}$) is measured at 0.5 *g*. (b) Measured RMS power output for three different accelerations for the 10 representative harvesters.

This could indicate that the variation in capacitance across the wafer is caused by both varying dielectric constants and PZT thicknesses.

While the capacitance and $F_{res}$ measurements give estimates of the variation of the mechanical parameters and the dielectric constant, the open circuit voltage measurements will provide information concerning variations in piezoelectric coefficients and quality factor since $V_{oc}=g_{31}\,\bar{\sigma}\,h_{PZT}$, where $g_{31}$ is the piezoelectric voltage coefficient, $\bar{\sigma}$ is the average induced stress in the PZT layer with thickness $h_{PZT}$. Besides being determined by mechanical properties, which also affects the resonant frequency, the average induced stress is related to the tip displacement at resonance and thus quality factor. The measured standard deviation relative to the average $V_{oc}$ is 32.2%, ignoring the two lowest and highest values gives a percentage of 27.4% which is still higher than what the variation in PZT thickness can account for. The majority of the variation in $V_{oc}$ is therefore believed to originate from either $g_{31}$ which is determined by how well the PZT thick film is polarized or the quality factor.

Except from the $V_{oc}$ measurements where the harvesters from the lower left corner of the wafer appears to have a general higher output, no significant wafer area tendencies are observed in the capacitance and $F_{res}$ measurements nor in-between all three measurements.

For the power output measurements the best uniformity in performance is observed in-between the three chips from the third quartile where the difference in power output is around or less than 1 μw for the three accelerations. Similar small variations are observed in bandwidth and quality factor. The resonant frequency varies from 325-344 Hz for the three chips which are considerably more than the measured bandwidth of around 6.8 Hz. The variation in power output of the three chips from the second quartile increases to around 3 μW difference at 1 *g*. For the first quartile chips, the variation is around 4.5 μW at 1 *g*. In average the first quartile devices harvest 30% and 36% less power than the second quartile devices at 0.5 *g* and 1 *g*, respectively. Third quartile devices perform 63% and 45% better than second quartile devices at 0.5 *g* and 1 *g*, respectively. Compared to the variation of the open circuit measurements this increased variation is expected since the output power is proportional to the voltage squared.

## 4. Conclusion

Measurements of the open circuit voltage for the 41 devices showed a relative difference of 32.6% between the standard deviation and average. Measurements of the capacitance and resonant frequency showed a relative difference between the standard deviation and average value of 4.3% and 2.9% respectively. This indicates that the main variation in open circuit voltage performance is caused by varying quality factor. Power output measurements showed good uniformity between chips with similar open circuit voltages from the high performance section. Decreasing uniformity was observed between chips from the section with lower open circuit voltage. A maximum power output of 39.3 μW was measured at 1 *g* for the best performing harvester. The power harvesting bandwidth was measured to 5-10 Hz, with the best performing harvesters having the lowest bandwidth. The average resonant frequency was measured to 333 Hz with a standard variation of 9.8 Hz.

## References

[1] S. Roundy, P. K. Wright, and J. Rabaey, *Computer Communications*, vol. 26, no. 11, pp. 1131–1144, Jul. 2003.

[2] A. Lei *et al.*, *Micro Electro Mechanical Systems (MEMS), 2011 IEEE 24th International Conference*, 2011, pp. 125 –128.

[3] R. Elfrink *et al.*, *J. Micromech. Microeng.*, vol. 19, no. 9, p. 094005, Sep. 2009.

[4] D. Shen *et al.*, *Sensors and Actuators A: Physical*, vol. 154, no. 1, pp. 103–108, Aug. 2009.